PERGAMON

International Journal of Solids and Structures 38 (2001) 8285–8304

INTERNATIONAL JOURNAL OF SOLIDS and STRUCTURES

www.elsevier.com/locate/ijsolstr

A model for the viscoelastic and viscoplastic responses of glassy polymers

Aleksey D. Drozdov *

Institute for Industrial Mathematics, 4 Yehuda Hanachtom Street, Beersheba 84311, Israel

Received 15 September 2000; in revised form 19 May 2001

Abstract

A constitutive model is derived for the viscoelastic and viscoplastic behavior of amorphous glassy polymers at isothermal loading with small strains. It is assumed that an amorphous polymer is strongly heterogeneous at the micro-scale. It is treated as an ensemble of cooperatively rearranging regions (CRR) which relax at random times as they are thermally agitated. CRRs are bridged by links (long chains which form less cohesive space between relaxing domains and transform the macro-strain in a specimen to rearranging regions). With the growth of strain, some links break (which reflects partial disentanglement of chains and scission of bonds in the less cohesive domains). This results in nucleation and aggregation of quasi-point defects (QPD) which provide some freedom for CRRs to displace with respect to each other. At the micro-level, the viscoelastic response of a polymer is reflected by rearrangement of CRRs, whereas the viscoplastic behavior is associated with coalescence of QPDs and creation of isolated islands of CRRs. Stress–strain relations for uniaxial loading are developed using the laws of thermodynamics. The constitutive equations are verified by comparison with experimental data for polycarbonate and poly(methyl methacrylate) at ambient temperature. Fair agreement is demonstrated between results of numerical simulation and observations in relaxation tests and in tests with constant strain rates.

Keywords: Amorphous polymers; Cooperative relaxation; Quasi-point defects; Viscoelasticity; Viscoplasticity

1. Introduction

This paper is concerned with modeling the viscoelastic and viscoplastic responses of amorphous glassy polymers at isothermal loading with small strains. We aim to develop constitutive equations which (i) correctly describe observations in uniaxial relaxation tests and in tests with constant strain rates, (ii) are based on a physically plausible concept at the micro-level, and (iii) account for the effect of plastic deformation on the characteristic times of relaxation.

Changes in elastic moduli and relaxation spectra of viscoelastic materials loaded in the sub-yield and post-yield regions are observed for several polymeric glasses. G'Sell et al. (1989) demonstrated that cyclic

* Tel.: +972-7-623-1313; fax: +972-7-623-1211.
E-mail address: aleksey@cs.bgu.ac.il (A.D. Drozdov).

0020-7683/01/$ - see front matter
PII: S0020-7683(01)00146-9

shear straining of polycarbonate (PC) with the maximal shear of the order of unity weakly affects the storage modulus, but dramatically increases the loss tangent in the entire α-region. Yoshioka et al. (1994) evidenced that at loading of poly(methyl methacrylate) (PMMA) with a constant strain rate, the storage modulus decreases and the loss tangent increases with the longitudinal strain. An increase in the loss tangent of PMMA with the strain level was confirmed by David et al. (1997) in experiments on plain strain compression. Changes in the elastic moduli begin in the sub-yield region and increase with the growth of strain. Govaert and Peijs (1995) showed that statically applied tensile stress caused an increase in the storage modulus and a decrease in the loss tangent for poly(vinyl alcohol) fibers. Pegoretti et al. (2000) observed a noticeable increase in the recovery rate for poly(ethylene terephthalate) with the growth of the maximal strain in loading–unloading tests with constant strain rates.

To the best of our knowledge, the effect of plastic deformation on relaxation spectra of glassy polymers has not yet been accounted for by existing constitutive models. The viscoelastoplastic response of glassy polymers is conventionally described using stress–strain relations based on the back-stress concept. The back stress (internal stress or equilibrium stress) is thought of as a measure of response of the surrounding material to plastic flow in locally transformed sites (shear micro-domains (SMD)). The theory of back stresses (which is purely phenomenological) may be applied to predict the viscoplastic behavior of polymers, as well as metals and other solids (Krempl, 1987). There are two approaches to the description of evolution of the back-stress tensor under loading. According to the first, nonlinear differential equations are introduced for the rate of changes in this tensor (Krempl et al., 1986; Krempl, 1996). A shortcoming of this method is that no rational explanation is provided why one or another nonlinear function is introduced in the governing equations and what is the physical meaning (at the micro-level) of adjustable parameters in the stress–strain relations. The other approach is based on the assumption that the response of the surrounding material (slowing down of the plastic flow in SMDs) may be described in the framework of the statistical theory of rubber elasticity (Haward and Thackray, 1968). The advantage of this concept is that it implies explicit formulas for the back stress (Boyce et al., 1988; Boyce and Arruda, 1990; Tomita and Tanaka, 1995; Spathis and Kontou, 1998). However, its physical basis (application of the theory of entropic elasticity to polymeric glasses) is questionable. In particular, the evolution of the back stress is based on the assumption that plastic flow implies alignment of long chains, which results in an increase in the equilibrium stress and a decrease in configurational entropy (which characterizes the level of disorder in a polymeric glass). The conclusion about a decrease in the configurational entropy contradicts observations (G'Sell et al., 1989) which evidence an increase in the configurational enthalpy of PC after several loading–unloading cycles in the post-yield region. The hypothesis about alignment of chains may be quite acceptable at large strains, but fitting adjustable parameters of the model to experimental data requires the alignment process to begin in the vicinity of the yield point (at strains of 5–10%). This result disagrees with birefringence measurements: changes in birefringence of polypropylene under uniaxial tension become evident only at the draw ratio exceeding two (Uehara et al., 1996), and small angle X-ray scattering, which does not reveal any changes in the diffraction index of polyethylene at strains $<20\%$.

The purpose of this study is to develop constitutive equations for the viscoelastic and viscoplastic behavior of glassy polymers which does not employ the concept of equilibrium stresses. Stress–strain curves for glassy polymers uniaxially loaded with constant strain rates are conventionally divided into four regions (Mangion et al., 1992): (i) a domain of a linear viscoelastic response, (ii) a region where the stress–strain curve reaches its maximum and begins to decrease (upper yield), (iii) an interval of strains where the stress decreases and reaches a plateau (lower yield), and (iv) a domain of a gradual increase in stress prior to failure. The study is confined to the response of amorphous polymers within the first two regions.

Our approach is based on the theory of cooperative relaxation (Adam and Gibbs, 1965). According to it, an amorphous polymer is treated as an ensemble of cooperatively rearranged regions (CRR) connected by links. A CRR is thought of as a globule consisting of scores of neighboring strands (Sollich, 1998) which change their position simultaneously because of large-angle reorientation of segments (Dyre, 1995). The

characteristic length of a relaxing region amounts to 1–2 nm in the vicinity of the glass transition temperature T_g (Arndt et al., 1997; Rizos and Ngai, 1999) and increases to about 4 nm at room temperature (Mermet et al., 1996). Cooperatively relaxing regions are identified with "isolated more cohesive regions" revealed by low-frequency Raman scattering of PC and PMMA loaded in the post-yield region (Achibat et al., 1995; Mermet et al., 1996).

In the stress-free state, all CRRs are connected with one another by links which ensure that the macro-strain in a specimen coincides with the micro-strains in relaxing regions. The links are thought of as long chains not included in CRRs (in the quasi-rubbery state) bridged by physical crosslinks, entanglements and van der Waals forces. Links between CRRs are associated with the penetrating "less cohesive space between more cohesive domains" (Mermet et al., 1996). With an increase in stress, some links break (which reflects partial disentanglement of chains and bond scission) providing excess "freedom" for relaxing regions (which can move with respect to each other). Failure of links consists of two stages (Coulon et al., 1986; G'Sell et al., 1989; Mangion et al., 1992): (i) nucleation of defects driven by annihilation of neighboring links (quasi-point defects (QPD) of high molecular mobility) and (ii) coalescence of QPDs which results in (partial) percolation of the ensemble of links and creation of shear micro-domains (temporary islands of CRRs which deform independently of the bulk material). Shear micro-domains are associated here with "fine slip bands" (David et al., 1997) where plastic flow occurs. Because healing (reformation) of links is not taken into account, the model is restricted to active programs of loading (without unloading).

The exposition is organized as follows. Section 2 focuses on the kinetics of rearrangement of CRRs and on thermodynamic potentials for an amorphous polymer. In Section 3 constitutive equations are derived for the viscoelastic and viscoplastic responses of glassy polymers using the laws of thermodynamics. The stress–strain relations are verified in Section 4 by comparing results of numerical simulation with experimental data in relaxation tests and in tests with constant strain rates on PC and PMMA. Some concluding remarks are formulated in Section 5.

2. A model for the viscoelastic response

In the phase space, a CRR is modeled as a point trapped in its potential well on the energy landscape (Dyre, 1995). At random times, the point hops from the bottom level of its potential well to higher energy levels as it is activated by thermal fluctuations. According to the transition-state theory (Goldstein, 1969), a CRR relaxes when it reaches some liquid-like (reference) energy level in a hop. The viscoelastic response of a polymer is modeled as successive rearrangement of CRRs trapped in potential wells with various depths.

The zero energy level on the energy landscape is chosen at the position of the reference state for a stress-free medium. The depth of a potential well with respect to this energy level is determined by its energy $w > 0$. It is assumed that the position of the liquid-like state is not fixed and coalescence of QPDs decreases the current reference energy level. Changes in the position of the liquid-like state with respect to the energy landscape are determined by the descent energy $\Omega(t)$. The function $\Omega(t)$ describes a decrease in relaxation times induced by viscoplastic deformation.

Denote by X_0 the number of CRRs per unit mass. The quantity X_0 is assumed to be constant and independent of the loading history. Let $X(t,\tau,w)$ be the current concentration of CRRs in cages with potential energy w which had last been rearranged before instant $\tau \leqslant t$. The function $X(t,\tau,w)$ entirely determines the rearrangement process. In particular, $X(t,t,w)$ is the concentration of CRRs (per unit mass) in traps with potential energy w at instant t. The conservation law for the numbers of CRRs with various energies implies that $X(t,t,w)$ is independent of time. This quantity is expressed in terms of the probability density of traps, $p(w)$, by the formula

$$X(t,t,w) = X_0 p(w). \tag{1}$$

Let $q(z)\mathrm{d}z$ be the probability for a CRR to reach (in a hop) an energy level belonging to the interval $[z, z+\mathrm{d}z]$. Referring to Bouchaud et al. (1998), we adopt the exponential distribution

$$q(z) = \alpha \exp(-\alpha z),$$

where α is a material constant. The probability to reach the reference state in an arbitrary hop reads

$$Q(t,w) = \int_{w-\Omega(t)}^{\infty} q(z)\mathrm{d}z = \exp[\alpha(\Omega(t)-w)].$$

Denote by Γ_0 the attempt rate (the average number of hops in a cage per unit time). The rate of rearrangement R is defined as the product of the attempt rate Γ_0 by the probability of reaching the liquid-like state in a hop Q,

$$R(t,w) = \Gamma(t)\exp(-\alpha w), \qquad \Gamma(t) = \Gamma_0 \exp[\alpha\Omega(t)]. \tag{2}$$

Equating the relative rates of rearrangement to the function R, we arrive at the differential equations

$$\frac{\partial X}{\partial t}(t,0,w) = -R(t,w)X(t,0,w), \qquad \frac{\partial^2 X}{\partial t\,\partial\tau}(t,\tau,w) = -R(t,w)\frac{\partial X}{\partial \tau}(t,\tau,w). \tag{3}$$

The physical meaning of Eq. (3) is discussed by Drozdov (1999). Integration of the first equality in Eq. (3) with the initial condition (1) implies that

$$X(t,0,w) = X_0 p(w)\exp\left[-\int_0^t R(s,w)\mathrm{d}s\right]. \tag{4}$$

Integrating the other equality in Eq. (3), we find that

$$\frac{\partial X}{\partial \tau}(t,\tau,w) = F(\tau,w)\exp\left[-\int_\tau^t R(s,w)\mathrm{d}s\right], \tag{5}$$

where

$$F(t,w) = \left.\frac{\partial X}{\partial \tau}(t,\tau,w)\right|_{\tau=t}. \tag{6}$$

According to Eq. (6), the function $F(t,w)$ equals the number of CRRs with energy w (per unit mass) returning to their cages after rearrangement at instant t. Neglecting the duration of a hop (a few picoseconds (Dyre, 1999)) compared to the characteristic time of relaxation in the sub-T_g region, we equate $F(t,w)$ to the number of CRRs (per unit mass) rearranged per unit time

$$F(t,w) = -\frac{\partial X}{\partial t}(t,0,w) - \int_0^t \frac{\partial^2 X}{\partial t\,\partial\tau}(t,\tau,w)\mathrm{d}\tau.$$

Substitution of expressions (3)–(5) into this equality results in the Volterra equation

$$F(t,w) = R(t,w)\left\{X_0 p(w)\exp\left[-\int_0^t R(s,w)\mathrm{d}s\right] + \int_0^t F(\tau,w)\exp\left[-\int_\tau^t R(s,w)\mathrm{d}s\right]\mathrm{d}\tau\right\}. \tag{7}$$

To solve Eq. (7), we set

$$Z(t,w) = F(t,w)\exp\left[\int_0^t R(s,w)\mathrm{d}s\right]. \tag{8}$$

It follows from Eqs. (7) and (8) that the function Z obeys the integral equation

$$Z(t,w) = R(t,w)\left[X_0 p(w) + \int_0^t Z(\tau,w)\mathrm{d}\tau\right]. \tag{9}$$

Eq. (9) implies that

$$Z(0,w) = X_0 p(w) R(0,w). \tag{10}$$

Differentiation of Eq. (9) with respect to time results in

$$\frac{\partial Z}{\partial t}(t,w) = \frac{\partial R}{\partial t}(t,w)\left[X_0 p(w) + \int_0^t Z(\tau,w)\mathrm{d}\tau\right] + R(t,w)Z(t,w).$$

Combining this equality with Eq. (9), we arrive at the differential equation

$$\frac{\partial Z}{\partial t}(t,w) = \frac{Z(t,w)}{R(t,w)}\frac{\partial R}{\partial t}(t,w) + R(t,w)Z(t,w). \tag{11}$$

We divide both parts of Eq. (11) by $Z(t,w)$, integrate the obtained equality from zero to t, and find that

$$\frac{Z(t,w)}{Z(0,w)} = \frac{R(t,w)}{R(0,w)}\exp\left[\int_0^t R(s,w)\mathrm{d}s\right].$$

This equality together with Eq. (10) implies that

$$Z(t,w) = X_0 p(w) R(t,w)\exp\left[\int_0^t R(s,w)\mathrm{d}s\right]. \tag{12}$$

Combining Eqs. (5), (8) and (12), we obtain

$$\frac{\partial X}{\partial \tau}(t,\tau,w) = X_0 p(w) R(\tau,w)\exp\left[-\int_\tau^t R(s,w)\mathrm{d}s\right]. \tag{13}$$

Relaxing regions are treated as linear elastic media with the mechanical energy

$$W_0(t,\tau,w) = \tfrac{1}{2}c\varepsilon_0^2(t,\tau). \tag{14}$$

Here c is the rigidity of a CRR and ε_0 is the strain from the stress-free configuration at instant τ (the last instant when the CRR was rearranged) to the deformed configuration at time t. For simplicity, we suppose that c is independent of depth, w, of the potential well where the CRR is trapped. The latter means that the parameter c is thought of as an average rigidity of CRRs in a virgin specimen.

Because a CRR totally relaxes when it reaches the liquid-like energy level, its stress-free state coincides with the deformed state of the ensemble of CRRs at the instant of rearrangement. This means that the strain ε_0 from the stress-free state of a relaxing region to its deformed state at time t is given by

$$\varepsilon_0(t,\tau) = \varepsilon(t) - \varepsilon(\tau), \tag{15}$$

where ε is the micro-strain in a CRR (which is assumed to be the same for different relaxing regions).

Summing the mechanical energies of CRRs and neglecting the energy of their interaction, we find from Eqs. (14) and (15) the strain energy density of a polymer (per unit mass)

$$W(t) = \frac{1}{2}c\left[\varepsilon^2(t)\int_0^\infty X(t,0,w)\mathrm{d}w + \int_0^t (\varepsilon(t)-\varepsilon(\tau))^2\mathrm{d}\tau\int_0^\infty \frac{\partial X}{\partial \tau}(t,\tau,w)\mathrm{d}w\right]. \tag{16}$$

Straining of glassy polymers in the yield region results in rather weak changes in temperature of specimens. For examples, we refer to experimental data for PC (Matsuoka and Bair, 1977) which demonstrate that temperature is altered by 0.6 K for tension with the strain rate 5.2×10^{-3} min^{-1} and the maximal strain 0.12 and by 0.75 K for shear with the strain rate 2.8×10^{-2} min^{-1} and the maximal strain 0.60. An increase in

temperature during necking of a PC specimen at uniaxial tension and its further stretching up to the maximal strain 0.35 with the strain rate 1.8×10^{-2} min^{-1} is estimated as 5 K (Zhou et al., 1995). Adopting the conventional value of the coefficient of thermal expansion for glassy PC, 2.2×10^{-4} K^{-1}, and PMMA, 2.6×10^{-4} K^{-1} (Schwarzl, 1990), we find that thermal expansion induced by the increase in temperature does not exceed 0.001, which is negligible compared to strains in the yield region. Measurements for several solid polymers demonstrate that changes in temperature in the range of about 30 K practically do not affect the specific heat κ (Liu and Harrison, 1987). Based on these observations, we propose the following expression for the free (Helmholtz) energy per unit mass:

$$\Psi = \Psi_0 + (S_0 - \kappa)(T - T_0) + \kappa T \ln \frac{T}{T_0} + W, \tag{17}$$

where Ψ_0 and S_0 are the free energy and the entropy (per unit mass) in the stress-free state at the reference temperature T_0, and κ is a constant.

Given a strain history $\varepsilon(t)$, expression (16) is determined by the only function: the probability density of traps with various depths, $p(w)$. To reduce the number of adjustable parameters, we confine ourselves to the quasi-Gaussian ansatz

$$p(w) = \frac{1}{\Sigma}\sqrt{\frac{2}{\pi}} \exp\left(-\frac{w^2}{2\Sigma^2}\right) \quad (w \geqslant 0), \qquad p(w) = 0 \quad (w < 0), \tag{18}$$

where Σ is an adjustable parameter (an analog of the standard deviation of energy for CRRs). An analog of Eq. (18) was suggested by Dyre (1995) in the framework of a random energy model.

3. A model for the viscoplastic response

Our main hypothesis is that nucleation and aggregation of QPDs are strongly distinguished in time: under active loading, nucleation of QPDs occurs at relatively small (but nonzero) stresses, whereas their coalescence and creation of shear micro-domains take place in the vicinity of the yield point, when the nucleation process is practically completed. This hypothesis is in agreement with observations on poly-amino-bismaleimide which demonstrate that QPDs appear clearly below the apparent yield point (Coulon et al., 1986). The nucleation process comes to its end in the sub-yield region when the number of QPDs is sufficiently high and creation of a new QPD requires more energy than aggregation of two existing QPDs.

This scenario implies that yield of a glassy polymer and its post-yield response are mainly associated with coalescence of defects. As a result, the nucleation stage may be excluded from the model, and its effect on the onset and growth of plastic strains may be accounted for by the introduction of some "average" characteristics of the material. We introduce two parameters: the effective strength of an ensemble of links, $g_0 > 0$, and the effective rigidity of a CRR, $c_0 > 0$. The strength g_0 is defined as the absolute value of the average stress that links can bear to prevent mutual displacements of CRRs at the stage of nucleation of defects (partial disentanglement of the "less cohesive space"). The rigidity c_0 is determined as the average rigidity of a CRR that correctly predicts the response of a polymer (at the macro-level) in the region of linear viscoelasticity (disentanglement and scission of chains in the less cohesive domain provide extra freedom for relaxing regions and make CRRs less tightened). During the nucleation process, g_0 and c_0 decrease with an increase in the number of quasi-point defects. Because the rate of increase in the number of QPDs is a nonmonotonic function of the current stress σ which vanishes at $\sigma = 0$ and $\sigma = \sigma_y$ (σ_y is an apparent yield stress) and which reaches its maximum within the interval $(0, \sigma_y)$, the parameters g_0 and c_0 are entirely determined by the total number of QPDs. The number of nucleated defects at the beginning of the stage of their aggregation is small for rapid loading and low temperatures (because the time required for the stress σ to reach its critical value σ_y is small, whereas the rate for nucleation of QPDs is finite) and it is

large for slow loading and relatively high temperatures (in the sub-T_g region). This implies that g_0 and c_0 should be decreasing functions of temperature and strain rate.

Referring to conventional theories of viscoplasticity, we postulate that the total macro-strain ϵ equals the sum of the viscoelastic strain ϵ_e and the viscoplastic strain ϵ_p. At the micro-level, the viscoelastic strain ϵ_e is associated with deformation of CRRs, whereas the viscoplastic strain ϵ_p reflects the displacement of CRRs with respect to one another. Assuming the macro-strain ϵ_e to be homogeneously distributed among relaxing regions, we set

$$\varepsilon = \epsilon_e,$$

which results in the formula

$$\varepsilon(t) = \epsilon(t) - \epsilon_p(t). \tag{19}$$

In the region of plastic flow (associated with coalescence of local defects), the strength of an ensemble of links, $g > 0$, monotonically decreases. The relative rate of the decrease in g is assumed to be proportional to the rate of viscoplastic strain,

$$\frac{1}{g}\frac{dg}{dt} = -k\left|\frac{d\epsilon_p}{dt}\right|, \tag{20}$$

where $k > 0$ is a material function. To simplify the model, we treat k is a constant which is independent of the loading history. To formulate the initial condition for Eq. (20), we suppose that the initial strength $g(0)$ coincides with the average strength of the ensemble of links at the end of the stage of nucleation of QPDs,

$$g(0) = g_0. \tag{21}$$

Eqs. (20) and (21) describe changes in the strength of less cohesive space between CRRs (which is determined by the average strength g) driven by the growth in the concentration of islands of quasi-point defects (which is characterized by the viscoplastic strain ϵ_p).

To describe the evolution of viscoplastic strain ϵ_p, we use the laws of thermodynamics. For uniaxial loading, the first law of thermodynamics implies that

$$\rho\frac{d\Phi}{dt} = \sigma\frac{d\epsilon}{dt} - \frac{\partial\chi}{\partial x} + \rho r, \tag{22}$$

where ρ is a constant mass density in the stress-free state at the reference temperature T_0, Φ is the internal energy per unit mass, σ is the stress, χ is the heat flux, and r is the heat supply per unit mass. The Clausius–Duhem inequality is given by

$$\rho\frac{dQ}{dt} = \rho\frac{dS}{dt} + \frac{\partial}{\partial x}\left(\frac{\chi}{T}\right) - \frac{\rho r}{T} \geqslant 0, \tag{23}$$

where S is the entropy and Q is the entropy production per unit mass. Bearing in mind that

$$\frac{\partial}{\partial x}\left(\frac{\chi}{T}\right) = \frac{1}{T}\frac{\partial\chi}{\partial x} - \frac{\chi}{T^2}\frac{\partial T}{\partial x},$$

and excluding the derivative $\partial\chi/\partial x$ from Eqs. (22) and (23), we find that

$$T\frac{dQ}{dt} = T\frac{dS}{dt} - \frac{d\Phi}{dt} + \frac{1}{\rho}\left(\sigma\frac{d\epsilon}{dt} - \frac{\chi}{T^2}\frac{\partial T}{\partial x}\right) \geqslant 0.$$

This inequality together with the conventional formula

$$\Phi = \Psi + ST,$$

implies that

$$T\frac{\mathrm{d}Q}{\mathrm{d}t}=S\frac{\mathrm{d}T}{\mathrm{d}t}-\frac{\mathrm{d}\Psi}{\mathrm{d}t}+\frac{1}{\rho}\left(\sigma\frac{\mathrm{d}\epsilon}{\mathrm{d}t}-\frac{\chi}{T^2}\frac{\partial T}{\partial x}\right)\geqslant 0. \tag{24}$$

The amount Q is split into the sum of two quantities,

$$Q=Q_{\mathrm{e}}+Q_{\mathrm{p}}, \tag{25}$$

where Q_{e} determines the entropy production induced by rearrangement of CRRs and Q_{p} describes the entropy production driven by plastic flow. For a steady-state plastic flow, the parameter Q_{p} is given by the conventional formula

$$Q_{\mathrm{p}}(t)=\int_0^t\frac{\mathrm{d}\Lambda}{\mathrm{d}\tau}(\tau)\frac{\mathrm{d}\tau}{T(\tau)}, \tag{26}$$

where

$$\Lambda(t)=\frac{1}{\rho}\int_0^{\epsilon_{\mathrm{p}}(t)}\sigma(\tau)\mathrm{d}\epsilon_{\mathrm{p}}(\tau), \tag{27}$$

is the plastic work per unit mass. For a transient regime of loading (in the vicinity of the yield point) when the stationary flow is not yet reached, Eq. (27) should be modified in such a way that in the limit of stationary plastic straining, the new formula turns into the conventional relationship. We assume that after the interval of transitory plastic deformation the rate of viscoplastic strain, $\dot{\epsilon}_{\mathrm{p}}=\mathrm{d}\epsilon_{\mathrm{p}}/\mathrm{d}t$, reaches the strain rate, $\dot{\epsilon}=\mathrm{d}\epsilon/\mathrm{d}t$, and the strength of an ensemble of links, g, vanishes,

$$\frac{\mathrm{d}\epsilon_{\mathrm{p}}}{\mathrm{d}t}\to\frac{\mathrm{d}\epsilon}{\mathrm{d}t},\qquad g\to 0\qquad (t\to\infty). \tag{28}$$

This implies that a modified expression for the plastic work may be taken in the form

$$\Lambda(t)=\frac{1}{\rho}\left[\int_0^{\epsilon_{\mathrm{p}}(t)}\left(\frac{\dot{\epsilon}_{\mathrm{p}}(\tau)}{\dot{\epsilon}(\tau)}\right)^{1/m}\sigma(\tau)\,\mathrm{d}\epsilon_{\mathrm{p}}(\tau)\pm\int_0^{\epsilon_{\mathrm{p}}(t)}g(\tau)\,\mathrm{d}\epsilon_{\mathrm{p}}(\tau)\right], \tag{29}$$

where m is a positive parameter. Eq. (29) implicitly presumes that the sign of the rate of plastic strain, $\dot{\epsilon}_{\mathrm{p}}$ coincides with the sign of the strain rate, $\dot{\epsilon}$. The first term in Eq. (29) determines the plastic work within the transient region (at $|\dot{\epsilon}_{\mathrm{p}}|<|\dot{\epsilon}|$ this work is less than the plastic work for the developed plastic flow). The other term in Eq. (29) equals the plastic work of the stress produced by nonbroken links between CRRs. Because the effective strength of links, g, is thought of as a positive quantity, the sign "+" in Eq. (29) stands for tension and the sign "−" for compression. It is worth noting that under condition (28), the last term in Eq. (29) tends to a constant which does not affect the differential inequality (24).

It follows from Eqs. (16), (17) and (19) (where the rigidity of a CRR, c, is replaced by the average rigidity, c_0) that

$$\frac{\mathrm{d}\Psi}{\mathrm{d}t}(t)=\left[S_0+c\ln\frac{T(t)}{T_0}\right]\frac{\mathrm{d}T}{\mathrm{d}t}(t)+\frac{\Upsilon(t)}{\rho}\left[\frac{\mathrm{d}\epsilon}{\mathrm{d}t}(t)-\frac{\mathrm{d}\epsilon_{\mathrm{p}}}{\mathrm{d}t}(t)\right]-J(t), \tag{30}$$

where

$$\Upsilon(t) = \rho c_0 \left[\big(\epsilon(t) - \epsilon_p(t)\big) \int_0^\infty X(t,0,w)\mathrm{d}w + \int_0^t \Big(\big(\epsilon(t) - \epsilon_p(t)\big) - \big(\epsilon(\tau) - \epsilon_p(\tau)\big) \Big) \mathrm{d}\tau \int_0^\infty \frac{\partial X}{\partial \tau}(t,\tau,w)\mathrm{d}w \right],$$

$$J(t) = \frac{1}{2} c_0 \left[\big(\epsilon(t) - \epsilon_p(t)\big)^2 \int_0^\infty R(t,w) X(t,0,w)\mathrm{d}w + \int_0^t \Big(\big(\epsilon(t) - \epsilon_p(t)\big) - \big(\epsilon(\tau) - \epsilon_p(\tau)\big) \Big)^2 \mathrm{d}\tau \right.$$
$$\left. \times \int_0^\infty R(t,w) \frac{\partial X}{\partial \tau}(t,\tau,w)\mathrm{d}w \right]. \tag{31}$$

Because R and X are nonnegative functions, Eq. (31) implies that the function $J(t)$ is nonnegative as well.

Substitution of Eqs. (25), (26), (29) and (30) into Eq. (24) results in

$$T(t)\frac{\mathrm{d}Q_e}{\mathrm{d}t}(t) = J(t) - \frac{\chi(t)}{\rho T^2(t)} \frac{\partial T}{\partial x}(t) + \left[S(t) - S_0 - \kappa \ln \frac{T(t)}{T_0} \right] \frac{\mathrm{d}T}{\mathrm{d}t}(t) + \frac{\sigma(t) - \Upsilon(t)}{\rho} \frac{\mathrm{d}\epsilon}{\mathrm{d}t}(t)$$
$$+ \frac{1}{\rho} \left[\Upsilon(t) - \sigma(t) \left(\frac{\dot\epsilon_p(t)}{\dot\epsilon(t)} \right)^{1/m} \mp g(t) \right] \frac{\mathrm{d}\epsilon_p}{\mathrm{d}t}(t) \geqslant 0.$$

Applying the conventional reasoning to this inequality (Coleman and Gurtin, 1967), we find that the coefficients at the derivatives $\mathrm{d}T/\mathrm{d}t$ and $\mathrm{d}\epsilon/\mathrm{d}t$ should vanish, which, together with Eq. (31), implies that

$$S(t) = S_0 + \kappa \ln \frac{T(t)}{T_0}, \sigma(t)$$
$$= \rho c_0 \left[\big(\epsilon(t) - \epsilon_p(t)\big) \int_0^\infty X(t,0,w)\mathrm{d}w + \int_0^t \Big(\big(\epsilon(t) - \epsilon_p(t)\big) - \big(\epsilon(\tau) - \epsilon_p(\tau)\big) \Big) \mathrm{d}\tau \int_0^\infty \frac{\partial X}{\partial \tau}(t,\tau,w)\mathrm{d}w \right]. \tag{32}$$

According to Eq. (32), the Clausius–Duhem inequality reads

$$T\frac{\mathrm{d}Q_e}{\mathrm{d}t} = J - \frac{\chi}{\rho T^2}\frac{\partial T}{\partial x} + \frac{1}{\rho}\left[\sigma \left(1 - \left(\frac{\dot\epsilon_p}{\dot\epsilon} \right)^{1/m} \right) \mp g \right] \frac{\mathrm{d}\epsilon_p}{\mathrm{d}t} \geqslant 0. \tag{33}$$

This inequality is satisfied for an arbitrary loading program, $\epsilon = \epsilon(t)$, provided that

1. the heat flux χ obeys the Fourier law with a positive thermal diffusivity λ,

$$\chi = -\lambda \frac{\partial T}{\partial x},$$

2. the last term in Eq. (33) vanishes.

The latter condition is tantamount to the law of plastic flow

$$\frac{\mathrm{d}\epsilon_p}{\mathrm{d}t}(t) = 0, \qquad |\sigma(t)| < g(t),$$
$$\frac{\mathrm{d}\epsilon_p}{\mathrm{d}t}(t) = \frac{\mathrm{d}\epsilon}{\mathrm{d}t}(t) \left[\frac{|\sigma(t)| - g(t)}{|\sigma(t)|} \right]^m, \qquad |\sigma(t)| \geqslant g(t). \tag{34}$$

The second equality in Eq. (34) is similar to the constitutive relation for the rate of plastic strain suggested by Krempl (1996) within the framework of the viscoplasticity theory based on overstress and by Hasan and Boyce (1995) based on the concept of thermomechanically activated inelastic flow. There is, however, an important difference between Eq. (34) and previous relations. Unlike Krempl (1996), Eq. (34) does not contain any additional nonlinear function of viscoplastic strain, whose experimental determination may be a complicated task. In contrast with Boyce et al. (1988) and Hasan and Boyce (1995), Eq. (34) provides a

power law for the rate of plastic strain (whereas previous studies employed exponential laws). Comparison of these two phenomenological laws (Zhang and Moore, 1997) demonstrates that the power law ensures better fitting of observations for glassy polymers.

Given a loading program $\epsilon = \epsilon(t)$, the stress $\sigma(t)$ is determined by Eq. (32), where the function $X(t,\tau,w)$ is found from Eqs. (4) and (13) and the function $\epsilon_p(t)$ obeys Eq. (34). Formulas (4) and (13) contain the function $R(t,w)$ which is determined in terms of the descent energy of the liquid-like state, Ω, by Eq. (2). The descent in the position of the reference state on the energy landscape is assumed to be proportional to the plastic work per unit volume,

$$\frac{d\Omega}{dt} = \zeta\sigma\frac{d\epsilon_p}{dt}, \qquad \Omega(0) = 0, \tag{35}$$

where ζ is an adjustable parameter. As a result, we arrive at the stress–strain relations determined by the quantities: Γ_0, Σ, g_0, k, m, ζ and $E_0 = \rho c_0 X_0$ (without loss of generality, we set $\alpha = 1$). The inverse to the attempt rate Γ_0 is the characteristic time of stress relaxation, Σ determines the relaxation spectrum, g_0 and E_0 characterize the strength of the ensemble of links and the elastic modulus at the end of the stage of nucleation of defects, k is the rate of decrease in the strength of less cohesive space driven by viscoplastic flow, m is the exponent in the power law (34) for the rate of viscoplastic strain, and ζ describes the effect of plastic flow on the relaxation spectrum. The number of adjustable parameters in the model is essentially less than that in conventional stress–strain relations for viscoelasticity and viscoplasticity of glassy polymers, see, e.g., Hasan and Boyce (1995), Krempl et al. (1986) and Spathis and Kontou (1998).

4. Comparison with experimental data

We begin with the analysis of a standard relaxation test with

$$\epsilon(t) = \begin{cases} 0, & t < 0, \\ \epsilon_0, & t > 0, \end{cases} \tag{36}$$

where ϵ_0 is essentially less than the yield strain ϵ_y. Assuming viscoplastic strains to vanish ($\epsilon_p = 0$, $\Omega = 0$), we substitute Eqs. (2), (4), (13) and (36) into Eq. (32) and find that

$$E(t) = E_0\int_0^\infty p(w)\exp[-\Gamma_0 t\exp(-w)]dw, \tag{37}$$

where $E(t) = \sigma(t)/\epsilon$ is the current Young modulus. Eqs. (18) and (37) are determined by three constants: E_0, Γ_0 and Σ.

To find these parameters, we approximate experimental data in a tensile relaxation test on PC with the strain $\epsilon_0 = 0.01$ at ambient temperature. For a description of specimens and the experimental procedure, we refer to Colucci et al. (1997). Given E_0, the parameters Γ_0 and Σ are determined using the steepest-descent procedure. The initial Young modulus E_0 is found by the least-squares algorithm. Fig. 1 demonstrates fair agreement between observations and results of numerical simulation.

The fitting procedure is repeated for PMMA loaded with the strain $\epsilon_0 = 0.005$ at room temperature. To increase the interval of time for the tensile relaxation test, we match the relaxation master curve obtained by shifts of experimental data measured at various aging times. A detailed description of specimens and the experimental procedure is provided by Cizmecioglu et al. (1981). Fig. 2 shows good correspondence between observations and results of numerical analysis. Adjustable parameters of the model found by fitting observations in relaxation tests for PC and PMMA are listed in Table 1.

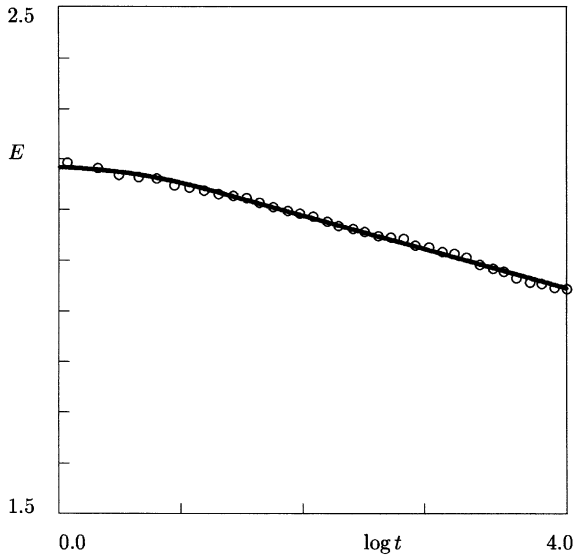

Fig. 1. The elastic modulus E (GPa) versus time t (s) for PC in a tensile relaxation test with the strain $\epsilon_0 = 0.01$. (○) experimental data (Colucci et al., 1997). (—) results of numerical simulation.

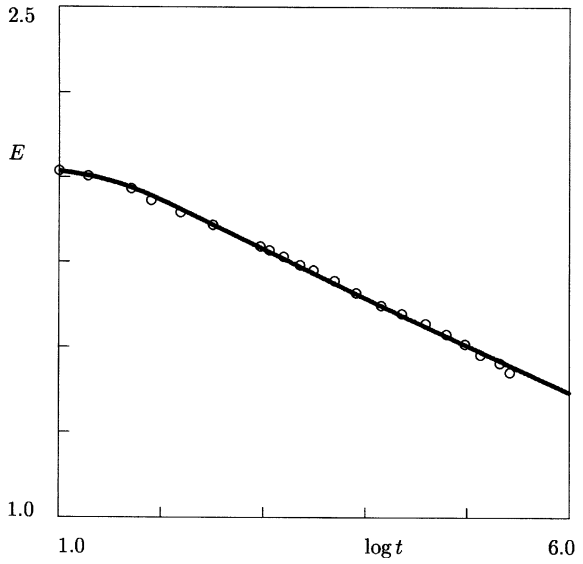

Fig. 2. The elastic modulus E (GPa) versus time t (s) for PMMA in a tensile relaxation test with the strain $\epsilon_0 = 0.005$. (○) experimental data (Cizmecioglu et al., 1981). (—) results of numerical simulation.

We proceed with the approximation of experimental data in uniaxial tests with a constant strain rate,

$$\epsilon(t) = \begin{cases} 0, & t < 0, \\ \dot{\epsilon}_0 t, & t > 0. \end{cases} \tag{38}$$

Substitution of Eqs. (2), (4), (13) and (38) into Eq. (32) results in

Table 1
Adjustable parameters found by matching observations in relaxation tests

Polymer	E_0 (GPa)	Γ_0 (s^{-1})	Σ
PC	2.19	0.150	58.0
PMMA	2.03	0.024	25.4

Table 2
Adjustable parameters for two grades of PC found by matching observations in tests with constant strain rates

Reference	Loading	$\dot{\epsilon}_0$ (min^{-1})	g_0	k	ζ
Tervoort et al. (1996)	Tension	0.006	10.9	82.0	0.7
Tervoort et al. (1996)	Tension	0.06	11.5	82.0	0.7
Tervoort et al. (1996)	Tension	0.6	12.0	82.0	0.7
Quinson et al. (1996)	Compression	0.1	16.6	70.0	3.1

$$\sigma(t) = E_0\Bigg\{(\dot{\epsilon}_0 t - \epsilon_p(t))\int_0^\infty p(w)\exp\left(-\Gamma_0\int_0^t \exp(\Omega(s)-w)\mathrm{d}s\right)\mathrm{d}w + \Gamma_0\int_0^t(\dot{\epsilon}_0(t-\tau)-(\epsilon_p(t)-\epsilon_p(\tau)))\mathrm{d}\tau\int_0^\infty \exp(\Omega(\tau)-w)p(w) \times \exp\left[-\Gamma_0\int_\tau^t \exp(\Omega(s)-w)\mathrm{d}s\right]\mathrm{d}w\Bigg\}. \tag{39}$$

To reduce the number of adjustable parameters, we set $m = 4$ for all experimental data. Our numerical analysis reveals that the stress–strain curves are weakly affected by the quantity m.

We begin with fitting observations for PC at room temperature. For a description of the experimental procedure, see Tervoort et al. (1996). The adjustable parameters E_0, Γ_0 and Σ are taken from fitting observations in the relaxation test (Table 1). First, we match experimental data in a test with the maximal strain rate $\dot{\epsilon}_0 = 0.01\ s^{-1}$. The quantities g_0, k and ζ are found by the trial-and-error method to ensure the best approximation of experimental data. Afterwards, we fix the values of k and ζ (Table 2) and match observations in other tests using the only adjustable parameter g_0. Fig. 3 demonstrates fair agreement between experimental data and results of numerical simulation. The effect of strain rate $\dot{\epsilon}_0$ on the parameter g_0 is shown in Fig. 4. Experimental data are fairly well approximated by the function

$$g_0 = a_0 + a_1 \log \dot{\epsilon}_0, \tag{40}$$

where the parameters a_i are found by the least-squares technique.

To assess the level of plastic strain, we repeat calculations for PC in a uniaxial compressive test at ambient temperature. The experiment consists of loading with the strain rate $\dot{\epsilon}_0 = 0.1\ min^{-1}$, rapid unloading with the strain rate $\dot{\epsilon}_0 = 1.0\ min^{-1}$, waiting for a time Δt in the stress-free state, and measurement of the residual strain ϵ_r. A detailed description of the experimental procedure can be found in Quinson et al. (1996). To approximate the stress–strain curve, we use the values of E_0, Γ_0 and Σ determined in the relaxation test (Table 1). The parameters g_0, k and ζ found by using the trial-and-error method are listed in Table 2. Fig. 5 demonstrates good agreement between results of numerical analysis and observations. Small deviations between the experimental data and the results of simulation at strains exceeding 0.15 may be ascribed to the geometrical nonlinearity of deformation and alignment of chain segments, the issues which are beyond the scope of the present study. The viscoplastic strain ϵ_p is plotted versus the longitudinal strain ϵ in Fig. 6 which shows that the viscoplastic strain is extremely small in the region of linear viscoelasticity and dramatically grows in the post-yield region (in accordance with the intuitive picture of viscoplastic

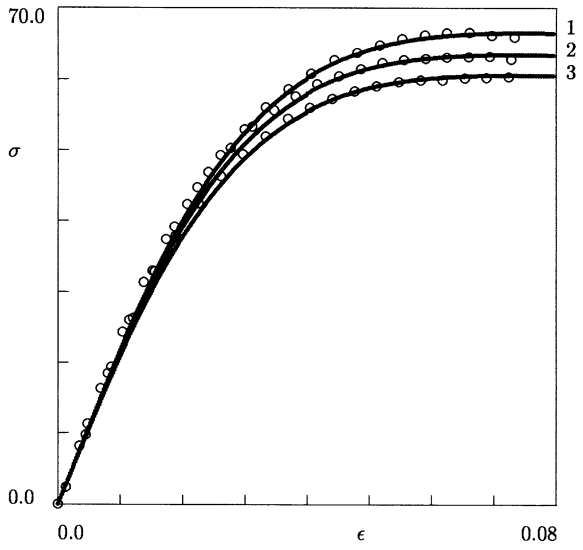

Fig. 3. Tensile stress σ (MPa) versus tensile strain ϵ for PC in a test with the strain rate $\dot{\epsilon}_0$ (s^{-1}). (○) experimental data (Tervoort et al., 1996). (—) results of numerical simulation. Curve 1: $\dot{\epsilon}_0 = 10^{-2}$; curve 2: $\dot{\epsilon}_0 = 10^{-3}$; curve 3: $\dot{\epsilon}_0 = 10^{-4}$.

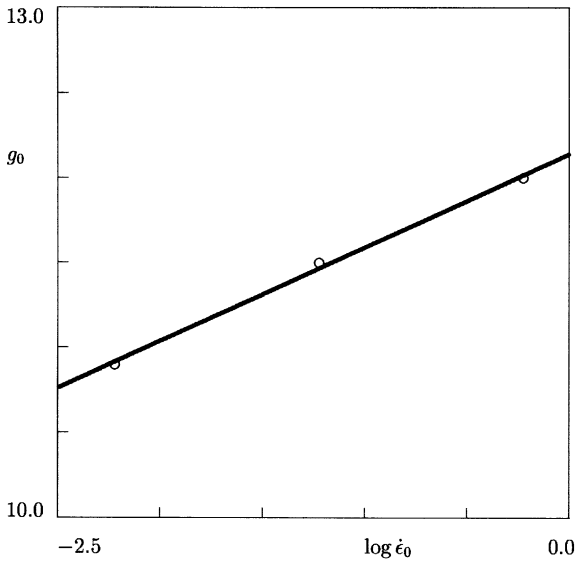

Fig. 4. The average strength of links at the beginning of the stage of coalescence of defects g_0 (MPa) versus the strain rate $\dot{\epsilon}_0$ (min^{-1}) for PC. (○) treatment of observations (Tervoort et al., 1996). (—) approximation of the experimental data by Eq. (40) with $a_0 = 12.14$ and $a_1 = 0.55$.

deformation). The parameters k and ζ found by fitting data for the two grades of PC are relatively close to each other (Table 2). For example, the difference in k is 14.6% only. The discrepancies in g_0 and ζ are higher; they may be associated with the difference in the straining state (tension versus compression), as well as with the difference in the molecular weight for these two grades of PC.

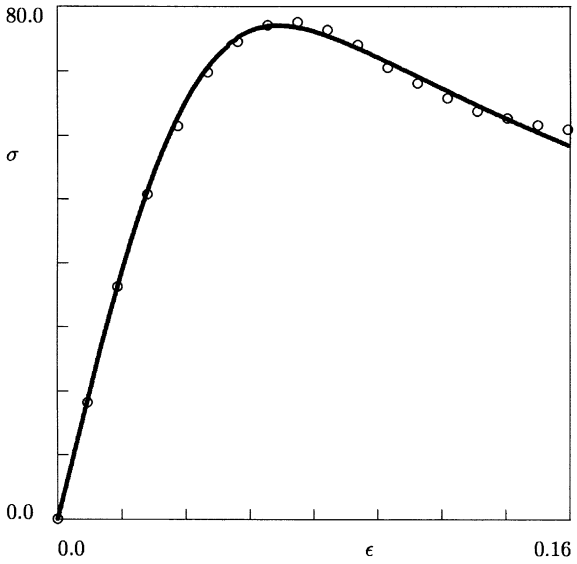

Fig. 5. Compressive stress σ (MPa) versus compressive strain ϵ for PC in a test with the strain rate $\dot{\epsilon}_0 = 0.1$ min^{-1}. (○) experimental data (Quinson et al., 1996). (—) results of numerical simulation.

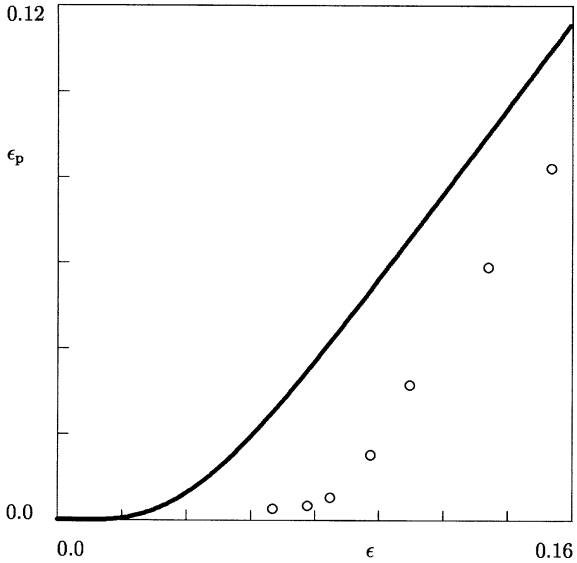

Fig. 6. Viscoplastic compressive strain ϵ_p versus compressive strain ϵ for PC in a test with the strain rate $\dot{\epsilon}_0 = 0.1$ min^{-1}. (—) results of numerical simulation. (○) residual strains after unloading with the strain rate $\dot{\epsilon}_0 = 1.0$ min^{-1} and $\Delta t = 10$ min of recovery (Quinson et al., 1996).

For comparison, observations are presented for the residual strain after unloading and recovery for $\Delta t = 10$ min. Fig. 6 reveals that the slope of the curve $\epsilon_p(\epsilon)$ is close to that for the experimental curve $\epsilon_r(\epsilon)$. The deviations between results of numerical analysis and measurements may be explained by recovery after unloading. Their level is in quantitative agreement with data for high density polyethylene (Zhang and

Moore, 1997) which show that recovery after unloading even for $\Delta t = 1$ min results in changes in the residual strains by 0.03 (the same level of discrepancy between observations and numerical results which is observed in Fig. 6).

We proceed with the approximation of stress–strain curves for PMMA in compressive tests with constant strain rates at ambient temperature. First, observations presented by Berthoud et al. (1999) are matched with the help of the parameters Γ_0 and Σ found by fitting experimental data in the relaxation test (Table 1). The quantities E_0, g_0, k and ζ are determined from the condition of the best fit of experimental data. The constants k and ζ are found in the test with the highest strain rate $\dot{\epsilon} = 0.01$ s^{-1} and are employed without changes to match data in tests with other strain rates. Any stress–strain curve is approximated by using only two adjustable parameters, E_0 and g_0. Fig. 7 shows fair agreement between experimental data and results of numerical simulation for strain rates in the interval from 10^{-4} to 10^{-2} s^{-1}.

The initial Young modulus, E_0, and the strength of links at the beginning of the stage of coalescence of defects, g_0, are plotted versus the strain rate $\dot{\epsilon}_0$ in Fig. 8. Experimental data are fairly well approximated by Eq. (40) and the phenomenological equation

$$E_0 = b_0 + b_1 \log \dot{\epsilon}_0. \tag{41}$$

The constants a_i and b_i in Eqs. (40) and (41) are calculated by the least-squares method.

Formulas (40) and (41) coincide with the conventional relations for the description of the effect of strain rate on the yield stress in glassy polymers (Bauwens-Crowet, 1969; Bauwens-Crowet et al., 1973). These equations are in agreement with the proposed scenario for nucleation of defects: rapid loading provides insufficient time for creation of QPDs which implies that the number of defects at the beginning of the stage of their coalescence is relatively small. This fact, in turn, results in a rather high strength of links and a rather large initial elastic modulus. On the contrary, slow loading implies that a large number of QPDs are nucleated which implies a decrease in the strength of links and initial Young's modulus of the bulk material. It should be stressed that Eqs. (40) and (41) are merely phenomenological and may be employed to match observations within a limited range of strain rates only.

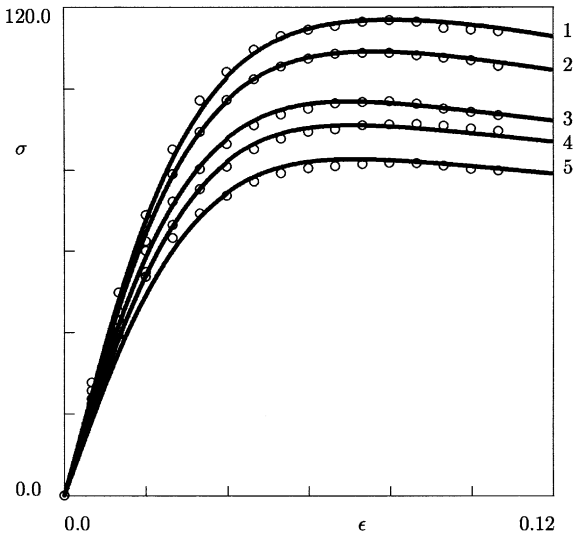

Fig. 7. Compressive stress σ (MPa) versus compressive strain ϵ for PMMA in a test with the strain rate $\dot{\epsilon}_0$ (s^{-1}). (○) experimental data (Berthoud et al., 1999). (—) results of numerical simulation. Curve 1: $\dot{\epsilon} = 10^{-2}$; curve 2: $\dot{\epsilon} = 5 \times 10^{-3}$; curve 3: $\dot{\epsilon} = 10^{-3}$; curve 4: $\dot{\epsilon} = 5 \times 10^{-4}$; curve 5: $\dot{\epsilon} = 10^{-4}$.

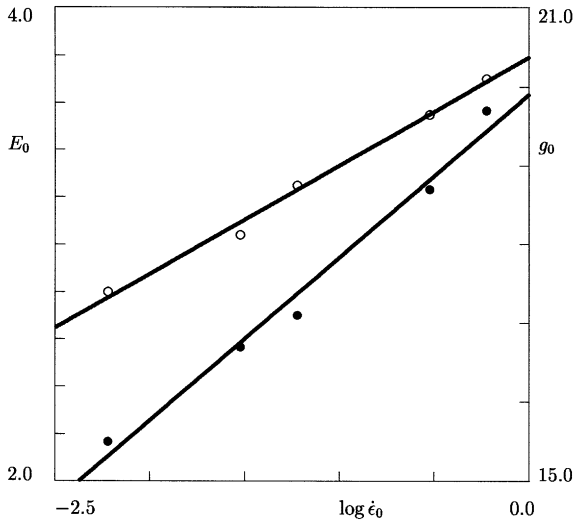

Fig. 8. The elastic modulus E_0 (GPa) (○) and the strength of links g_0 (MPa) (●) at the beginning of the stage of coalescence of defects versus the strain rate $\dot{\epsilon}_0$ (min^{-1}) for PMMA. Symbols: treatment of observations (Berthoud et al., 1999). (—) approximation of the experimental data by Eqs. (40) and (41) with $a_0 = 19.90$, $a_1 = 2.07$ and $b_0 = 3.70$, $b_1 = 0.46$.

Fair fitting of experimental data is established for PC when the initial Young modulus E_0 is taken from observations in the relaxation test, while for PMMA the quantity E_0 is treated as a function of the strain rate $\dot{\epsilon}_0$. This conclusion is in qualitative agreement with experimental data in dynamic mechanical tests that demonstrate that cyclic plastic loading weakly affects the storage modulus of PC (Figs. 3 and 5 in G'Sell et al. (1989)), whereas the storage modulus of PMMA dramatically decreases in the post-yield region (Figs. 1 and 2 in Yoshioka et al. (1994)). To explain this discrepancy, we refer to Xiao et al. (1994) where it is shown that PC is a type II polymer that is relatively ductile and undergoes extensive shear yielding at ambient temperature, whereas PMMA is a type I polymer that is relatively brittle and undergoes crazing. The difference in the mechanical response of these polymers may be ascribed to main-chain motion in PC which is highly restricted by entanglements between side groups in PMMA.

At first sight, the fact that the parameters E_0 and g_0 (which are conventionally thought of as material constants) are affected by the strain rate, $\dot{\epsilon}_0$, seems as a shortcoming of the model. It is worth noting, however, that the elastic modulus E_0 is expressed in terms of the rigidity, c_0, by the formula $E_0 = \rho c_0 X_0$, whereas the average rigidity of a CRR, c_0, and the average strength of an ensemble of links, g_0, are determined as appropriate characteristics of a glassy polymer at the end of the stage of nucleation of QPDs. This implies that the parameters E_0 and g_0 are treated within the model not as material constants for a virgin specimen, but as characteristics of a preconditioned polymer, whose dependence on the rate of loading at the stage of nucleation of defects seems quite natural.

To assess the level of plastic strains, we approximate experimental data in a uniaxial compressive test on PMMA with the strain rate $\dot{\epsilon}_0 = 0.1$ min^{-1} at room temperature. A detailed description of the experimental procedure is provided by Quinson et al. (1996). The same algorithm of fitting is employed as for the experimental data exposed in Berthoud et al. (1999). Fig. 9 demonstrates excellent agreement between observations and results of numerical simulation. The parameters E_0, k and ζ found by approximation of measurements for the two grades of PMMA are quite close to each other (Table 3). The viscoplastic strain ϵ_p is plotted versus the longitudinal strain ϵ in Fig. 10. The results of numerical simulation are in qualitative agreement with the graph of the function $\epsilon_p(\epsilon)$ calculated for PC (Fig. 6). The slope of the experimental curve $\epsilon_r(\epsilon)$ coincides with that for the theoretical dependence $\epsilon_p(\epsilon)$. As in the case of PC, the discrepancies

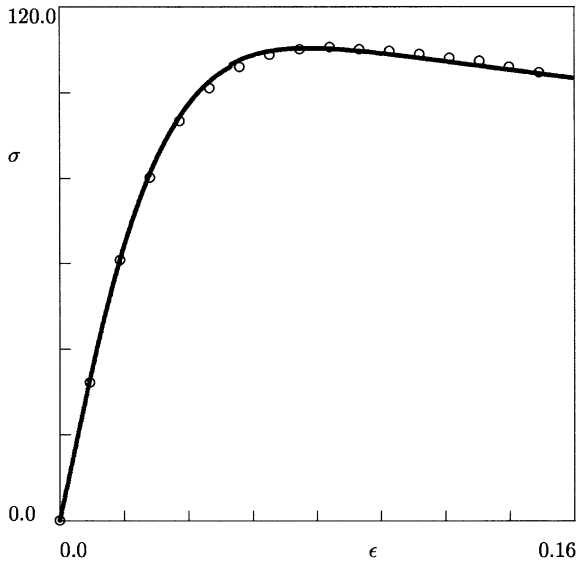

Fig. 9. Compressive stress σ (MPa) versus compressive strain ϵ for PMMA in a test with the strain rate $\dot{\epsilon}_0 = 0.1$ min^{-1}. (○) experimental data (Quinson et al., 1996). (—) results of numerical simulation.

Table 3
Adjustable parameters for two grades of PMMA found by matching observations in compressive tests with constant strain rates

Reference	$\dot{\epsilon}_0$ (min^{-1})	E_0 (GPa)	g_0	k	ζ
Berthoud et al. (1999)	0.006	2.80	15.5	74.0	0.40
Berthoud et al. (1999)	0.03	3.04	16.7	74.0	0.40
Berthoud et al. (1999)	0.06	3.25	17.1	74.0	0.40
Berthoud et al. (1999)	0.3	3.55	18.7	74.0	0.40
Berthoud et al. (1999)	0.6	3.70	19.7	74.0	0.40
Quinson et al. (1996)	0.1	3.56	18.8	70.0	0.25

between observations and results of numerical analysis may be ascribed to strain recovery after unloading. At first glance, the divergence should not be so large because of the small waiting time after unloading ($\Delta t = 5$ s). It is noteworthy, however, that at relatively large viscoplastic strains, the characteristic rate of relaxation drastically increases, see Eq. (35), which implies that even 5 s of recovery is sufficient for substantial changes in residual strains. To confirm this statement, we refer to data for polyethylene (Zhang and Moore, 1997) which demonstrate that at the maximal strain of 0.15, $\Delta t = 4.3$ s of recovery in the unloading mode increases the residual strain from 0.078 to 0.125.

Results of numerical simulation for the viscoplastic strain are compared in Figs. 6 and 10 with residual strains after unloading and waiting for a time Δt. A natural question arises about the direct comparison of observations with the calculated values of residual strains. This comparison is, however, a cumbersome task because numerical analysis of residual strains requires the account for the influence of viscoplastic deformations on relaxation spectra of glassy polymers. The latter effect has not yet been examined in detail either experimentally or theoretically.

It is worth noting that the model parameters are fitted to experimental data in short-term tests (with the characteristic time of about 10^3 s). This implies that some interesting phenomena associated with (possible) mechanically induced aging of specimens (observed in experiments on rubbery polymers, see Clarke et al.

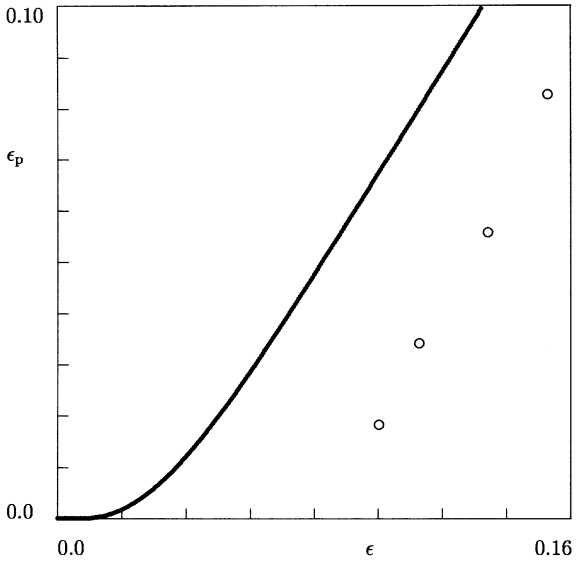

Fig. 10. Viscoplastic compressive strain ϵ_p versus compressive strain ϵ for PMMA in a test with the strain rate $\dot{\epsilon}_0 = 0.1$ min^{-1}. (—) results of numerical simulation. (○) residual strains after unloading with the strain rate $\dot{\epsilon}_0 = 1.0$ min^{-1} and $\Delta t = 5$ s of recovery (Quinson et al., 1996).

(2000)) remain beyond the scope of the present study. Our recent analysis of long-term observations (Drozdov and Kaschta, 2001) reveals, however, that the proposed approach provides fair agreement between results of numerical simulation and experimental data in long-term creep tests (with the duration of 10^6 s) on polystyrene and PMMA near the glass transition point.

5. Concluding remarks

A constitutive model has been derived for the viscoelastic and viscoplastic responses of amorphous glassy polymers at isothermal uniaxial loading with small strains. A polymer is treated as an ensemble of cooperatively rearranged regions bridged by less cohesive space. At the macro-level, thermally induced rearrangement of CRRs is associated with the viscoelastic behavior, whereas mechanically induced nucleation and coalescence of defects in the less cohesive domains (driven by disentanglement and scission of chains) reflect the viscoplastic response. Stress–strain relations are developed using the laws of thermodynamics. Constitutive equations contain a relatively small number of adjustable parameters (seven) that are found by fitting observations in standard relaxation tests and tests with constant strain rates. Fair agreement is demonstrated between results of numerical simulation and experimental data for PC and PMMA.

The paper exposes results of a preliminary study on the viscoelastic and viscoplastic behavior of glassy polymers. In particular, the kinetics of nucleation of quasi-point defects is disregarded and its effect on the mechanical response of solid polymers is replaced by phenomenological dependences of the influence of the strain rate on average quantities E_0 and g_0. Only experimental data at ambient temperature are used to determine material constants in the constitutive equations, which implies that the effect of temperature on adjustable parameters is not evaluated. The study is confined to rather simple loading programs: relaxation and uniaxial tension (compression) with constant strain rates, which means that the validity of the model to

predict observations in mechanical tests with more complicated (time dependent) protocols of straining has not yet been assessed. The stress–strain equations are verified by fitting observations only for two materials (PC and PMMA); the applicability of these relations for matching data for other glassy polymers remains unclear. These questions will be the subject of a subsequent work.

Acknowledgements

I am grateful to Dr. M. Ayzenberg for fruitful discussions. I express my sincere gratitude to Prof. E. Krempl who read a preliminary version of the paper and made some valuable suggestion. I would also like to thank anonymous reviewers for useful comments. The work is supported by the Israeli Ministry of Science through grant 1202-1-00.

References

Achibat, T., Boukenter, A., Duval, E., Mermet, A., Aboulfaraj, M., Etienne, S., G'Sell, C., 1995. Low-frequency Raman spectroscopy of plastically deformed poly(methyl methacrylate). Polymer 36, 251–257.

Adam, G., Gibbs, J.H., 1965. On the temperature dependence of cooperative relaxation properties in glass-forming liquids. J. Chem. Phys. 43, 139–146.

Arndt, M., Stannarius, R., Groothues, H., Hempel, E., Kremer, F., 1997. Length scale of cooperativity in the dynamic glass transition. Phys. Rev. Lett. 79, 2077–2080.

Bauwens-Crowet, C., 1969. The compression yield behaviour of polymethyl methacrylate over a wide range of temperatures and strain-rates. J. Mater. Sci. 8, 968–979.

Bauwens-Crowet, C., Bauwens, J.C., Homes, G., 1973. Tensile yield-stress behavior of glassy polymers. J. Polym. Sci. A-2 7, 735–742.

Berthoud, P., Baumberger, T., G'Sell, C., Hiver, J.-M., 1999. Physical analysis of the state- and rate-dependent friction law: static friction. Phys. Rev. B 59, 14313–14327.

Bouchaud, J.-P., Cugliandolo, L.F., Kurchan, J., Mezard, M., 1998. Out of equilibrium dynamics in spin glasses and other glassy systems. In: Young, A.P. (Ed.), Spin Glasses and Random Fields. World Scientific, Singapore, pp. 161–223.

Boyce, M.C., Arruda, E.M., 1990. An experimental and analytical investigation of the large strain compressive and tensile response of glassy polymers. Polym. Engng. Sci. 30, 1288–1302.

Boyce, M.C., Parks, D.M., Argon, A.S., 1988. Large inelastic deformation of glassy polymers. 1. Rate dependent constitutive model. Mech. Mater. 7, 15–33.

Cizmecioglu, M., Fedors, R.F., Hong, S.D., Moacanin, J., 1981. Effect of physical aging on stress relaxation of poly(methyl methacrylate). Polym. Engng. Sci. 21, 940–942.

Clarke, S.M., Elias, F., Terentjev, E.M., 2000. Ageing of natural rubber under stress. Eur. Phys. J. E 2, 335–341.

Coleman, B.D., Gurtin, M.E., 1967. Thermodynamics with internal state variables. J. Chem. Phys. 47, 597–613.

Colucci, D.M., O'Connell, P.A., McKenna, G.B., 1997. Stress relaxation experiments in polycarbonate: a comparison of volume changes for two commercial grades. Polym. Engng. Sci. 37, 1469–1474.

Coulon, G., Lefebvre, J.M., Escaig, B., 1986. The preyield evolution with strain of the work-hardening rate of glassy polymers (PABM resin). J. Mater. Sci. 21, 2059–2066.

David, L., Quinson, R., Gauthier, C., Perez, J., 1997. The role of anelasticity in high stress mechanical response and physical properties of glassy polymers. Polym. Engng. Sci. 37, 1633–1640.

Drozdov, A.D., 1999. A constitutive model for physical ageing in amorphous glassy polymers. Modelling Simul. Mater. Sci. Engng. 7, 1045–1060.

Drozdov, A.D., Kaschta, J., 2001. The viscoelastic and anelastic responses of amorphous polymers in the vicinity of the glass transition temperature. Preprint cond-mat/0105251.

Dyre, J.C., 1995. Energy master equation: a low temperature approach to Bässler's random-walk model. Phys. Rev. B 51, 12276–12294.

Dyre, J.C., 1999. Solidity of viscous liquids. Phys. Rev. E 59, 2458–2459.

Goldstein, M., 1969. Viscous liquids and the glass transition: a potential energy barrier picture. J. Chem. Phys. 51, 3728–3739.

Govaert, L.E., Peijs, T., 1995. Influence of applied stress and temperature on the deformation behaviour of high-strength poly(vinyl alcohol) fibres. Polymer 36, 3589–3592.

G'Sell, C., El Bari, H., Perez, J., Cavaille, J.Y., Johari, G.P., 1989. Effect of plastic deformation on the microstructure and properties of amorphous polycarbonate. Mater. Sci. Engng. A 110, 223–229.

Hasan, O.A., Boyce, M.C., 1995. A constitutive model for the nonlinear viscoelastic viscoplastic behavior of glassy polymers. Polym. Engng. Sci. 35, 331–344.

Haward, R.N., Thackray, G., 1968. The use of a mathematical model to describe stress–strain curves in glassy thermoplastics. Proc. R. Soc. London A 302, 453–472.

Krempl, E., 1987. Models of viscoplasticity. Some comments on equilibrium (back) stress and drag stress. Acta Mech. 69, 25–42.

Krempl, E., 1996. A small strain viscoplasticity theory based on overstress. In: Krausz, A.S., Krausz, K. (Eds.), Unified Constitutive Laws of Plastic Deformation, Academic Press, San Diego, pp. 281–318.

Krempl, E., McMahon, J.J., Yao, D., 1986. Viscoplasticity based on overstress with a differential growth law for the equilibrium stress. Mech. Mater. 5, 35–48.

Liu, T.-M., Harrison, I.R., 1987. Thermal effects in the necking of polymers. Polym. Engng. Sci. 27, 1399–1403.

Mangion, M.B.M., Cavaille, J.Y., Perez, J., 1992. A molecular theory for the sub-T_g plastic mechanical response of amorphous polymers. Phil. Mag. A 66, 773–796.

Matsuoka, S., Bair, H.E., 1977. The temperature drop in glassy polymers during deformation. J. Appl. Phys. 48, 4058–4062.

Mermet, A., Duval, E., Etienne, S., G'Sell, C., 1996. Effect of a plastic deformation on the nanostructure of polycarbonate: study by low-frequency Raman scattering. Polymer 37, 615–623.

Pegoretti, A., Guardini, A., Migliaresi, C., Ricco, T., 2000. Recovery of post-yield deformations in semicrystalline poly(ethylene-terephthalate). Polymer 41, 1857–1864.

Quinson, R., Perez, J., Rink, M., Pavan, A., 1996. Components of non-elastic deformation in amorphous glassy polymers. J. Mater. Sci. 31, 4387–4394.

Rizos, A.K., Ngai, K.L., 1999. Experimental determination of the cooperative length scale of a glass-forming liquid near the glass transition temperature. Phys. Rev. E 59, 612–617.

Schwarzl, F.R., 1990. Polymer Mechanik. Springer, Berlin.

Sollich, P., 1998. Rheological constitutive equation for a model of soft glassy materials. Phys. Rev. E 58, 738–759.

Spathis, G., Kontou, E., 1998. Experimental and theoretical description of the plastic behaviour of semicrystalline polymers. Polymer 39, 135–142.

Tervoort, T.A., Klompen, E.T.J., Govaert, L.E., 1996. A multi-mode approach to finite, three-dimensional, nonlinear viscoelastic behavior of polymer glasses. J. Rheol. 40, 779–797.

Tomita, Y., Tanaka, S., 1995. Prediction of deformation behavior of glassy polymers based on molecular chain network model. Int. J. Solids Struct. 32, 3423–3434.

Uehara, H., Yamazaki, Y., Kanamoto, T., 1996. Tensile properties of highly syndiotactic polypropylene. Polymer 37, 57–64.

Xiao, C., Jho, J.Y., Yee, A.F., 1994. Correlation between the shear yielding behavior and secondary relaxations of bisphenol A polycarbonate and related copolymers. Macromolecules 27, 2761–2768.

Yoshioka, S., Usada, H., Nanzai, Y., 1994. Variation of dynamic viscoelasticity during yielding and post-yield relaxation in a glassy polymer. J. Non-Cryst. Solids 172–174, 765–770.

Zhang, C., Moore, I.D., 1997. Nonlinear mechanical response of high density polyethylene. 1: Experimental investigation and model evaluation. Polym. Engng. Sci. 37, 404–413.

Zhou, Z., Chudnovsky, A., Bosnyak, C.P., Sehanobish, K., 1995. Cold-drawing (necking) behavior of polycarbonate as a double glass transition. Polym. Engng. Sci. 35, 304–309.